

Beam-target reversal symmetry in antiproton-neutron interactions in flight

E. Gold, G. C. Mason, G. I. Opat, K. R. Parker,* J. W. G. Wignall, G. J. Chapman, J. N. DeRoach, P. A. King, A. G. Klein, L. J. Martin, and S. N. Tovey

School of Physics, University of Melbourne, Parkville, Victoria, Australia 3052

(Received 18 March 1977)

A symmetry, applicable to the $\bar{p}n$ system, called "beam-target reversal symmetry," is derived from the conservation of G parity and is tested using data from an in-flight $\bar{p}d$ bubble-chamber exposure. Beam-target reversal symmetry predicts that for $\bar{p}n$ interactions, both inclusive and exclusive, all reaction products which are eigenstates of G parity have forward-backward-symmetric angular distributions in the center-of-mass frame. The prediction is consistent with experimental event distributions presented.

I. INTRODUCTION

The G -parity operation, invented by Lee and Yang,¹⁻³ is well known, and conservation of G parity in the strong interaction is customarily assumed. However, as for other hadronic symmetries such as $SU(2)$, tests of G -parity conservation have been limited predominantly to low energies and to exclusive processes, for example, $\rho \rightarrow 3\pi$ decay.⁴

In this paper we apply the hypothesis of G -parity conservation to a particular system: the antiproton-neutron interaction in flight. We find some readily testable predictions which apply at *all* energies, some of them *inclusively*, and which, to our knowledge, have not been pointed out before. Further, we present experimental evidence which is consistent with such predictions.

In Sec. II of this paper we develop the theoretical consequences of G -parity conservation applied to the $\bar{p}n$ system. The major prediction is the forward-backward symmetry in the center-of-mass frame of those final-state mesons that are eigenstates of G parity. In Sec. III the predictions of beam-target reversal symmetry are compared with our experimental data, and in Sec. IV we draw the conclusion that such a symmetry, and hence G -parity conservation, is supported by this experiment. In addition, we discuss briefly the consequences of G -parity conservation for K mesons, as well as some $SU(3)$ generalizations of G parity that could be tested if $\bar{\Sigma}^-$ or possibly $\bar{\Sigma}^+$ beams become available.

II. THEORY

Consider the scattering of antiproton and neutron into a final state f , and let

$$\langle f|S|\bar{p}(a),n(b)\rangle \quad (1)$$

denote the scattering matrix element, where the labels a, b are composite indices specifying both

momentum and helicity. The G -parity operation⁵ applied to the initial state yields

$$G|\bar{p}(a),n(b)\rangle = |n(a),\bar{p}(b)\rangle \quad (2)$$

from which we note that, apart from an interchange of helicities, the roles of beam and target have been reversed. For the full matrix element

$$\langle f|S|\bar{p}(a),n(b)\rangle = \langle f|G^\dagger S|\bar{p}(b),n(a)\rangle, \quad (3)$$

where we have used Eq. (2) and the fact that G is both unitary and conserved. We now apply this result to exclusive and inclusive processes.

A. Exclusive reactions

If the final state $|f\rangle$ of Eq. (3) is an eigenstate of G parity having eigenvalue η_f , then

$$\langle f|S|\bar{p}(a),n(b)\rangle = \eta_f \langle f|S|\bar{p}(b),n(a)\rangle. \quad (4)$$

It follows from Eq. (4) that for any differential cross section

$$d\sigma(a,b) = d\sigma(b,a), \quad (5)$$

and if we make explicit the momenta and helicities, $a = (\vec{p}_a, h_a)$, $b = (\vec{p}_b, h_b)$, we may average over helicities to give the cross-section relation appropriate to unpolarized beam and target:

$$d\sigma(\vec{p}_a, \vec{p}_b) = d\sigma(\vec{p}_b, \vec{p}_a). \quad (6)$$

We call this result "beam-target reversal symmetry."

The physical significance of Eq. (6) is illustrated in Fig. 1: The probability of ejection of a given particle into the forward hemisphere of the center-of-mass frame equals that into the same polar solid-angle element in the backward hemisphere, i.e.,

$$\frac{d\sigma}{d\Omega}(\cos\theta) = \frac{d\sigma}{d\Omega}(-\cos\theta). \quad (7)$$

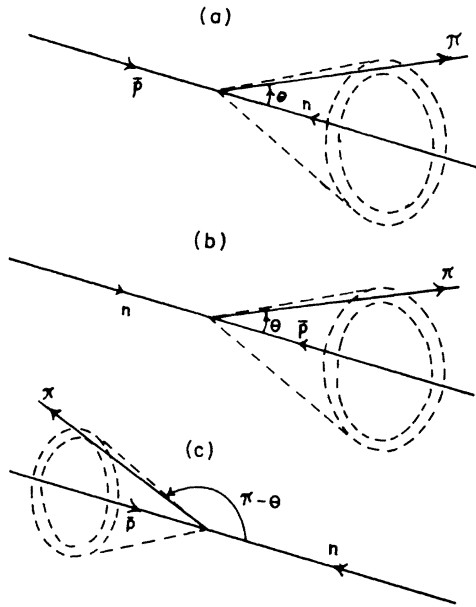


FIG. 1. The reaction $\bar{p}n \rightarrow$ pions in the center-of-mass frame; the pion is representative of the final-state particles; the others are not shown. (b) differs from (a) by the application of G parity to initial and final states; (c) differs from (b) only by a rotation in space.

B. Inclusive reactions

Let a_d^\dagger be the creation operator for one of the detected particles in an inclusive $\bar{p}n$ reaction and let $|r\rangle$ denote a possible state of the remaining undetected particles. We consider only the case in which each of the detected particles is an eigenstate of G , but we do not require $|r\rangle$ to be an eigenstate of G . Thus

$$\begin{aligned} G|f\rangle &= G\left(\prod_d a_d\right)^\dagger |r\rangle \\ &= \eta_d \left(\prod_d a_d\right)^\dagger G|r\rangle \\ &= \eta_d \left(\prod_d a_d\right)^\dagger |r'\rangle, \end{aligned} \quad (8)$$

where η_d is the total G parity of the detected particles, and

$$|r'\rangle \equiv G|r\rangle. \quad (9)$$

The set of states $\{|r'\rangle\}$ only differs from the set $\{|r\rangle\}$ in order and possibly in phase. Thus with an appropriate summation \sum_r ,

$$\sum_r |r\rangle \langle r| = \sum_r |r'\rangle \langle r'|. \quad (10)$$

Using Eqs. (3), (8), (9), and (10) it follows that

$$\sum |\langle f|S|\bar{p}(a), n(b)\rangle|^2 = \sum |\langle f|S|\bar{p}(b), n(a)\rangle|^2. \quad (11)$$

From Eq. (11) the inclusive-cross-section result follows readily, namely

$$\left(\prod_d D_d\right)\sigma(a, b) = \left(\prod_d D_d\right)\sigma(b, a), \quad (12)$$

where

$$D_d \equiv E_d d/d^3 p_d. \quad (13)$$

Equation (12) shows the beam-target reversal symmetry for $\bar{p}n$ inclusive reactions. In summary, if each of the set of detected particles in a $\bar{p}n$ reaction is an eigenstate of G parity, then all particle distributions should show beam-target reversal symmetry.

C. ρ - ω interference

We now consider the interference between the processes

$$\bar{p}n \rightarrow \rho^0 X, \quad \rho^0 \rightarrow \pi^+ \pi^-, \quad (14)$$

$$\bar{p}n \rightarrow \omega^0 X, \quad \omega^0 \rightarrow \pi^+ \pi^-. \quad (15)$$

The ω^0 decay into two pions, being electromagnetic, violates G -parity conservation.

The overall amplitude for reactions (14) and (15) is given by

$$\begin{aligned} A(a, b) &= T(\pi^+ \pi^-; \rho^0) T(\rho^0 X; \bar{p}(a)n(b)) \\ &\quad + T(\pi^+ \pi^-; \omega^0) T(\omega^0 X; \bar{p}(a)n(b)). \end{aligned} \quad (16)$$

Each term in Eq. (16) is the product of a production and a decay amplitude (in a self-evident notation).

For simplicity, let us assume that X is an eigenstate of G . Then remembering that $\eta_\rho = 1$, $\eta_\omega = -1$, it follows from Eq. (3) that

$$\begin{aligned} A(b, a) &= \eta_x [T(\pi^+ \pi^-; \rho^0) T(\rho^0 X; \bar{p}(a)n(b)) \\ &\quad - T(\pi^+ \pi^-; \omega^0) T(\omega^0 X; \bar{p}(a)n(b))]. \end{aligned} \quad (17)$$

Comparison of Eqs. (16) and (17) shows that if ρ - ω interference is constructive in the forward direction, it will be destructive in the backward direction (or vice versa). The amplitude $T(\pi^+ \pi^-; \omega^0)$, since it is electromagnetic in origin, is small, so that the interference term in the cross section will also be small. The situation is illustrated in Fig. 2.

We make three comments:

(i) ρ - ω interference cannot be seen in $\bar{p}n$ interactions if the direction of production is integrated over. This conclusion is not true for $\bar{p}p$ reactions, where the interference is seen.⁶

(ii) ρ - ω interference cannot be seen in $\bar{p}n$ inter-

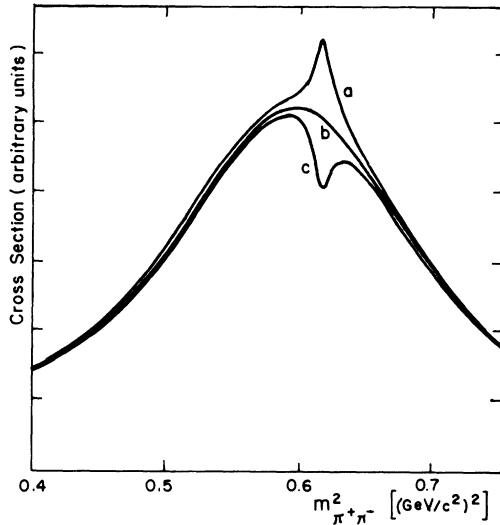


FIG. 2. The appearance of ρ - ω interference in a $\pi^+\pi^-$ effective mass-squared plot for $\bar{p}n \rightarrow$ pions. In the case of constructive interference in the forward direction, curve *a* represents ρ - ω forward at some polar angle θ , while curve *c* corresponds to ρ - ω backward at the angle $\pi-\theta$. Curve *b* is the mass plot obtained in the transverse direction, $\theta = \pi/2$, where the interference term is zero.

actions at zero momentum, because the beam-target direction is not defined.

(iii) The conclusions for ρ - ω interference hold also for inclusive ρ - ω production. In this case the results follow from the technique implied in Eqs. (3), (8), (9), (10), and (11) rather than the requirement that X be an eigenstate of G .

III. EXPERIMENTAL RESULTS

The data presented here come from several exposures of the deuterium-filled BNL 30-in. bubble chamber to beams of antiprotons, covering a momentum range from 350 to 930 MeV/ c in 10 steps. About half of the 240 000 pictures were taken in the 550-MeV/ c bin. We have combined all momentum bins to produce a sample of 13 700 kinematically fitted $\bar{p}n$ annihilations into 3, 4, 5, and 6 pions.

A. Forward-backward symmetry

We have examined all possible single-pion angular distributions, as well as those of many dipion combinations, from the 3-, 4-, 5-, and 6-pion final states. For the three-pion final state, events fall into two classes: those with seen proton stubs and those without. For those events without seen proton stubs, the unconstrained stub momentum was taken as zero with an uncertainty $\Delta p_x = \Delta p_y = \Delta p_z = 50$ MeV/ c . Events from both classes satis-

fying a 4C kinematic fit uniquely were accepted into the final three-pion sample. No difference was detected between the two classes of events. For the four-, five-, and six-pion final states, only events with a measured proton stub satisfying a unique kinematic fit were accepted. A total of some 3500 events satisfied the above criteria.

For each angular distribution examined, we have calculated a χ^2 statistic corresponding to the hypothesis that the distribution is forward-backward symmetric.^{7a} Not one distribution failed this symmetry test at the 95% confidence level.^{7b}

For economy of space, we present in Figs. 3 and 4 a representative selection of angular distributions: the π^- distribution for each of the four final-state multiplicities. Forward-backward symmetry is evident in the figures which include values of χ^2 calculated as above.

Symmetry is evident not only for individual final-state particles, for which the angular distributions are in some cases fairly flat, but also for exclusive processes exhibiting structure. Figure 5 shows data for the quasi-two-body processes $\bar{p}n \rightarrow \rho^0\pi_1^-$, and $\bar{p}n \rightarrow f^0\pi_1^-$, where the ρ^0 and f^0 in fact include a substantial background, being defined simply by mass selections in the $\pi^+\pi_2^-$ spectrum (Fig. 6).

An alternative statement of beam-target reversal symmetry is that partial waves that violate G parity should be absent; that is, no coherent odd and even amplitudes can exist simultaneously, and indeed simple fits to our data using Legendre polynomials are consistent with that prediction. By way of example, two three-pion distributions exhibiting much structure are shown in Fig. 7, to-

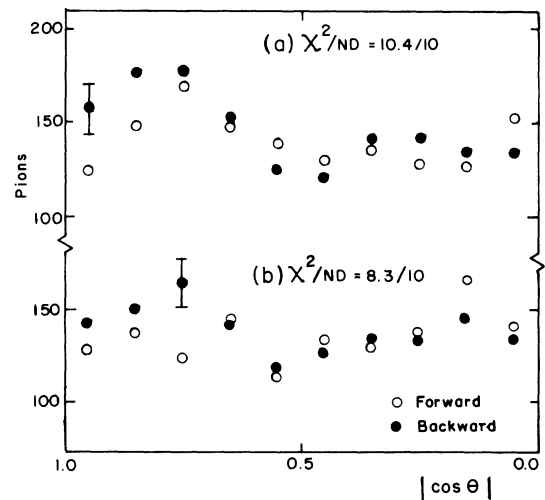


FIG. 3. Forward and backward c.m. angular distributions of π^- from (a) $\bar{p}n \rightarrow \pi^+\pi^-\pi^-$, (b) $\bar{p}n \rightarrow \pi^+\pi^-\pi^-\pi^0$.

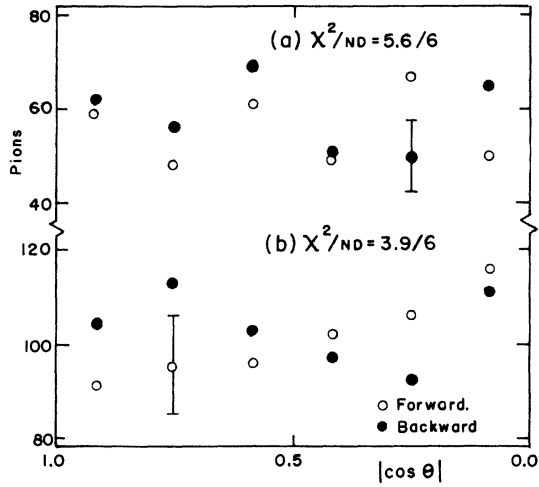


FIG. 4. Forward and backward c.m. angular distributions of π^- from (a) $\bar{p}n \rightarrow \pi^+ \pi^+ \pi^- \pi^- \pi^- \pi^-$, (b) $\bar{p}n \rightarrow \pi^+ \pi^+ \pi^- \pi^- \pi^- \pi^- \pi^0$.

gether with coefficients of fitted Legendre polynomials. In each case, a good fit can be obtained using even terms only. A full partial-wave analysis for the three-pion final state is the subject of a separate paper currently in preparation.

While the above distributions are consistent with beam-target reversal symmetry, the predicted symmetry is a stronger one than is tested by the usual center-of-mass cosine distribution alone. That is, if a center-of-mass system is defined relative to initial-state particles, with the beam direction specifying the polar axis, tests can be

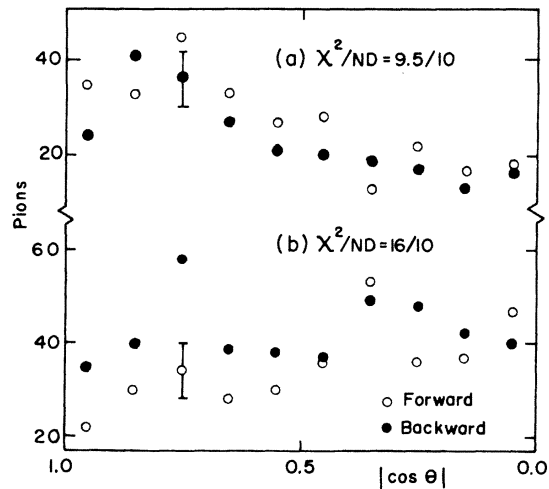


FIG. 5. Forward and backward c.m. angular distributions of $\pi_1^+ \pi_2^-$ from $\bar{p}n \rightarrow \pi^+ \pi_1^- \pi_2^+$ with $m(\pi^+ \pi_2^-)$ (a) in the ρ^0 band, (b) in the f^0 band.

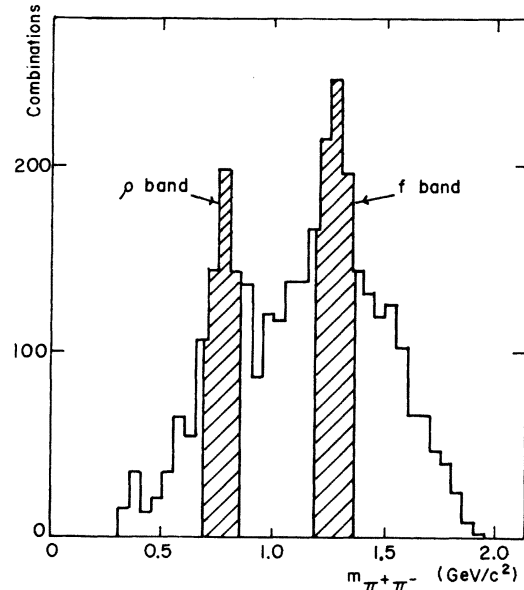


FIG. 6. Mass selection used for the data of Fig. 5.

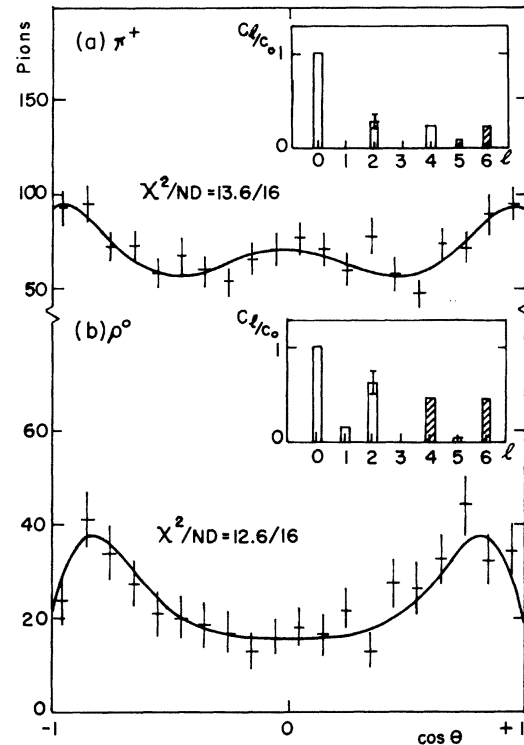


FIG. 7. Angular distributions and coefficients of fitted Legendre polynomials for (a) π^+ from $\bar{p}n \rightarrow \pi^+ \pi^- \pi^-$, (b) π^- from $\bar{p}n \rightarrow \pi^+ \pi^- \pi^- \pi^- \pi^- \pi^- \pi^0$. Negative coefficients are shown shaded. The smooth curves and χ^2 values relate to fits using even terms only.

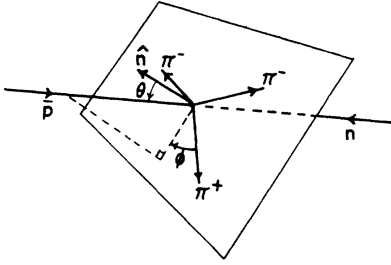


FIG. 8. The center-of-mass frame used to test Eq. (18), for the reaction $\bar{p}n \rightarrow \pi^+ \pi^- \pi^-$. The x axis is along the π^+ direction and the z axis is specified by the normal $\vec{\pi}_1 \times \vec{\pi}_2$ where, for definiteness of sense, $m(\pi^+ \pi_1^-) > m(\pi^+ \pi_2^-)$.

made only of the polar symmetry; azimuthal event distributions are inherently isotropic, for unpolarized beam and target, because a reference axis cannot be defined. A more sensitive test of beam-target reversal symmetry can be made over a full 4π sr if a center-of-mass frame is defined relative to the final-state particles.

We choose, as an example, the center-of-mass frame shown in Fig. 8 for the reaction $\bar{p}n \rightarrow \pi^+ \pi_1^- \pi_2^-$. The x axis lies along the π^+ direction, and the z axis is normal to the plane containing the final-state pions. For definiteness of sense in specifying the normal, we calculate $\vec{\pi}_1^- \times \vec{\pi}_2^-$ where $m(\pi^+ \pi_1^-) > m(\pi^+ \pi_2^-)$. Beam-target reversal symmetry applied to this system requires that the antiproton differential cross section into any element of solid angle, $d\Omega$, equals that into the diametrically opposite element, i.e.,

$$\frac{d\sigma}{d\Omega}(\cos\theta, \phi) = \frac{d\sigma}{d\Omega}(-\cos\theta, \phi + \pi), \quad (18)$$

where again averaging over initial-state helicities

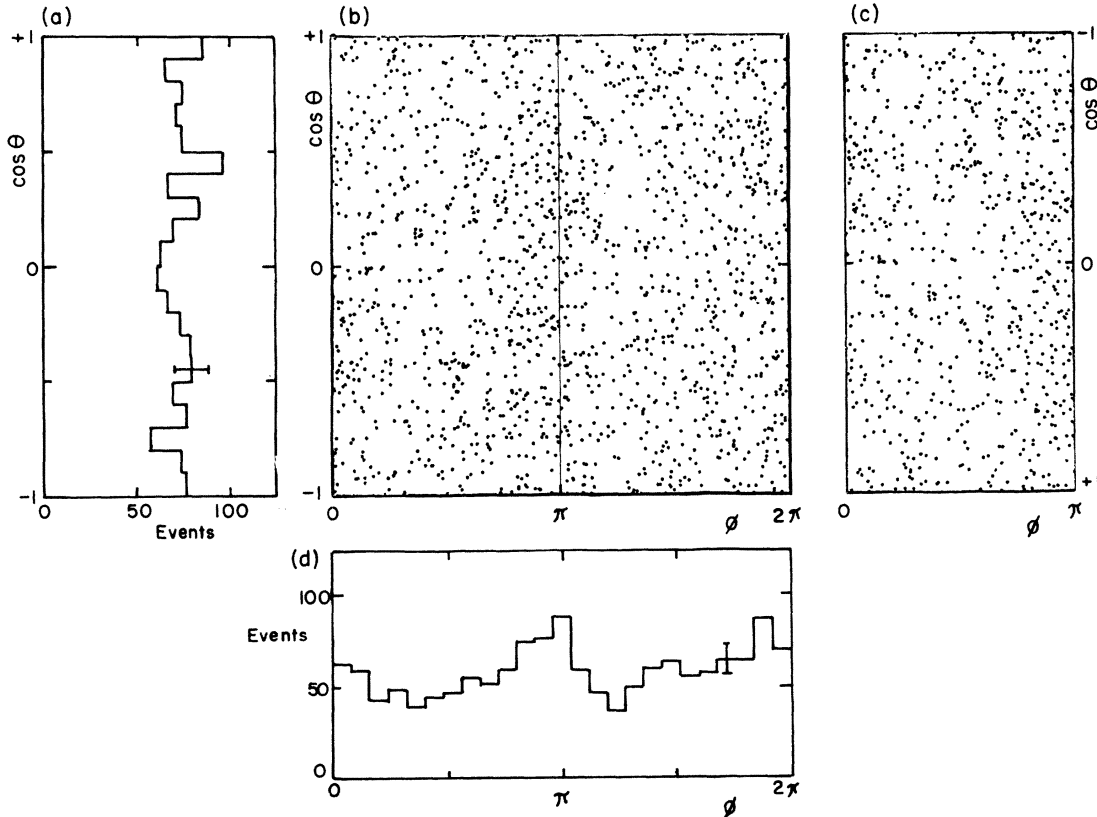


FIG. 9. Angular distribution of \bar{p} in the c.m. frame of Fig. 8 for $\bar{p}n \rightarrow \pi^+ \pi^- \pi^-$. The scatter plot (c) is the left-hand half of (b) with $\cos\theta$ coordinates reversed. Thus if beam-target reversal symmetry holds, (c) and the right-hand half of (b) should be identical: This is most readily seen if the left half of (b) is covered over. (a) and (d) are the $\cos\theta$ and ϕ projections, respectively.

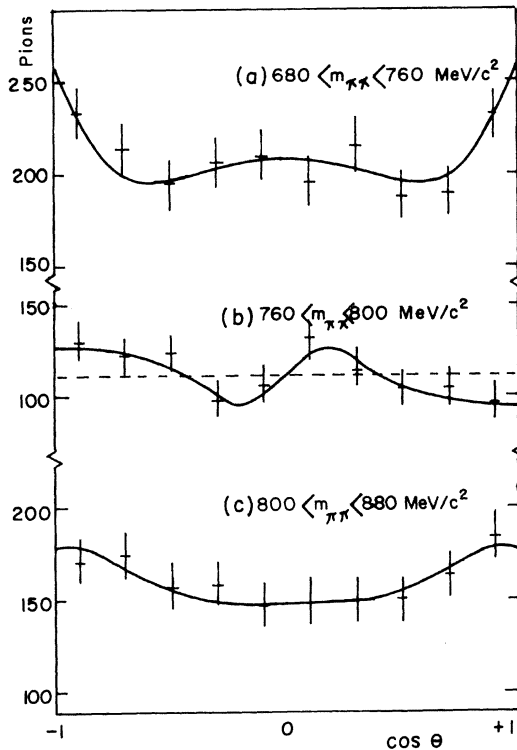


FIG. 10. Center-of-mass angular distributions for dipions ($\pi^+ \pi^-$) from the reaction $\bar{p}n \rightarrow \pi^+ \pi^- \pi^- \pi^0$ in a “ $\rho-\omega$ ” band and two adjacent mass bins (uncut sample). The smooth curves have no theoretical significance.

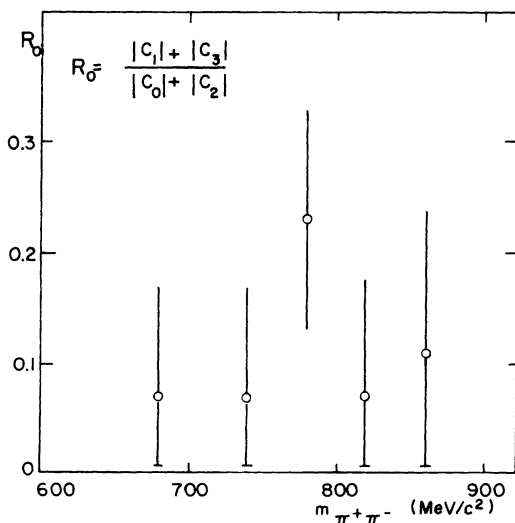


FIG. 11. The ratio $R_0 = \text{odd coefficients/even coefficients}$ of low-order Legendre polynomials fitted to the dipion ($\pi^+ \pi^-$) angular distributions from $\bar{p}n \rightarrow \pi^+ \pi^- \pi^- \pi^0$ reactions, as a function of dipion mass. The ratio is calculated using a sum of magnitudes only.

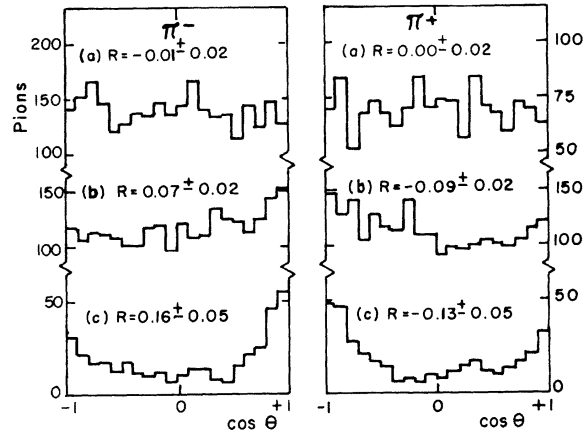


FIG. 12. Center-of-mass angular distributions of π^- and π^+ from the reactions (a) $\bar{p}n \rightarrow \pi^+ \pi^- \pi^- \pi^0$ (this experiment), (b) $\bar{p}p \rightarrow \pi^+ \pi^+ \pi^- \pi^-$ near $940 \text{ MeV}/c^2$ (Ref. 10), (c) $\bar{p}p \rightarrow \pi^+ \pi^+ \pi^- \pi^-$ at $5.7 \text{ GeV}/c$ (Ref. 11). The ratio R is defined in Ref. 8(a). The symmetry exhibited in (b) and (c) is that of charge-conjugation invariance which predicts that the π^+ and π^- distributions should be reflections of each other.

is accomplished if beam and target are unpolarized.

To test the equivalence of the experimental distribution at diametrically opposite points we divided each hemisphere into 32 zones of equal solid angle and performed a χ^2 test similar to the one above. We find $\chi^2/\text{ND} = \frac{31}{32}$ for the data shown in Fig. 9, indicating that the distribution is quite consistent with the symmetry predicted, as shown by a comparison of Figs. 9(b) and 9(c). A similar test for isotropy failed at the 99% confidence level, as is to be expected from the projections in Fig. 9, particularly in ϕ . Thus the diametric symmetry holds despite a large amount of structure, i.e., the presence of several partial waves.

B. $\rho-\omega$ interference

For the reaction $\bar{p}n \rightarrow \pi^+ \pi^- \pi^- \pi^0$, events have been selected into three dipion ($\pi^+ \pi^-$) mass bins: a “ $\rho-\omega$ ” band $40 \text{ MeV}/c^2$ wide centered on the ω^0 mass, and two contiguous bins; Fig. 10 shows their angular distributions. Employing the same test statistic as above, the distribution in the “ $\rho-\omega$ ” region is *not* consistent with symmetry at the 95% confidence level despite being consistent with isotropy. It is worth stressing that the G -parity argument predicts not *asymmetry* but *antisymmetry* (on top of a symmetric background) in the mass region of the ω^0 . Although statistically poor, there is slight evidence in Fig. 10 that the angular distribution has an antisymmetric part in the “ $\rho-\omega$ ” band, while being consistent with symmetry in adjacent mass regions.

That this effect occurs only in the region of the ω^0 mass is illustrated in Fig. 11, where, as a simple measure of the antisymmetric part, we have plotted, as a function of dipion mass, the ratio of odd to even coefficients required to fit Legendre polynomials to the center-of-mass angular distributions.

IV. DISCUSSION AND COMMENTS

The experimental angular distributions discussed in Sec. III are in many cases far from isotropic, indicating the presence of several partial waves. Nevertheless, they are *all* consistent with beam-target reversal symmetry. It is unfortunate that the limited statistics of this experiment, together with an inherent arbitrariness of parametrization, preclude a very precise estimate of any G -parity violating amplitude. The asymmetry parameter, R ,^{8a} affords an approximate but model-independent estimate of the G -violating amplitude.^{8b} For both the three-pion and four-pion data of this experiment we find $R < 0.04$ at the 90% confidence level. Thus in each case we expect the G -violating amplitude to be less than $\sim 4\%$ of the G -conserving amplitude. More stringent limits have been set previously near the 1% level; however, they are model-dependent and apply to particular decay processes such as $\rho \rightarrow 3\pi$ decay⁴ and $\omega \rightarrow 2\pi$ decay.⁹ The suggestion, although weak, of a ρ - ω interference effect in our data is consistent with the electromagnetic decay of the latter. In summary, we note that the model-independent forward-backward symmetry has not been explicitly tested before, and that to the extent that beam-target reversal symmetry is satisfied in this experiment, G -parity conservation is supported for $\bar{p}n$ interactions.

We suggest three related experimental areas in which beam-target reversal symmetry can be more rigorously tested. First, a high-energy analysis in comparison with $\bar{p}p$ reactions should better reveal the effect of the G -parity constraint, and could be made inclusively. The reactions $\bar{p}p \rightarrow$ pions do *not* show forward-backward symmetry^{10,11}; a "leading-particle" effect is present, as

shown in Fig. 12. That is, the charged-pion angular distributions are peaked forward in the direction of the initial-state particle that has the same charge. Furthermore, the effect becomes more pronounced at higher energies. This asymmetry, combined with our results, strongly suggests that partial waves present in $\bar{p}p$ annihilations, for which the G -parity constraint does not apply, are dynamically excluded by G -parity conservation in $\bar{p}n$ interactions. Second, we expect a full partial-wave analysis of any high-statistics $\bar{p}n$ reaction channel to demonstrate the absence of G -parity-forbidden waves. Third, a high-statistics analysis of the possible ρ - ω interference effect should complement analogous studies of $\bar{p}p$ reactions.⁶

Finally, we comment on G -parity conservation for K mesons, and a generalization of G parity to U spin and V spin.

(a) As

$$G|K^0\rangle = i|K^-\rangle, \\ G|\bar{K}^0\rangle = i|K^+\rangle,$$

Eq. (3) predicts that the K^0 (\bar{K}^0) angular distribution is the same as the "reflected" K^- (K^+) angular distribution for any final-state kaons. Further, triangle inequalities follow for K_S^0, K^+, K^- cross sections.

(b) (i) If I_1 in Ref. 5 is replaced by U_1 then, in $\bar{\Sigma}^+p$ reactions, final-state $K^0, \bar{K}^0, K_L^0, K_S^0$ particles should all show beam-target reversal symmetry, in a manner analogous to the pions from $\bar{p}n$ annihilations. These predictions form a sensitive test of the extent to which SU(3) is a good symmetry for strong interactions.

(ii) In a similar way, if I_1 in Ref. 5 is replaced by V_1 then, in $\bar{\Sigma}^-n$ reactions, any final-state K^+, K^- particles should show beam-target reversal symmetry.

ACKNOWLEDGMENTS

We are grateful to the Brookhaven National Laboratory for the use of its bubble-chamber facilities, to H. J. Stephen and her scanning and measuring staff for their careful work on the bubble-chamber film, and to the Australian Research Grants Committee for financial support.

*Now at Department of Theoretical Physics, University of Oxford, England.

¹T. D. Lee and C. N. Yang, *Nuovo Cimento* **3**, 749 (1956).

²A. Pais and R. Jost, *Phys. Rev.* **87**, 871 (1952).

³L. Michel, *Nuovo Cimento* **10**, 319 (1953).

⁴G. S. Abrams, K. W. J. Barnham, W. R. Butler, D. G. Coyne, G. G. Goldhaber, B. H. Hall, and J. Mac-

Naughton, *Phys. Rev. D* **4**, 653 (1971).

⁵Our definition of G coincides with that of G. Källén, *Elementary Particle Physics* (Addison-Wesley, Reading, Mass., 1964). The charge-conjugation operator is so chosen that $CI_2 = I_+C$, $C_2J = -I_3C$, and $G \equiv C \cdot \exp i\pi I_1$.

⁶W. W. M. Allison, W. A. Cooper, T. Fields, and D. S. Rhines, *Phys. Rev. Lett.* **24**, 618 (1970).

^{7a}We calculated the χ^2 statistic corresponding to the hypothesis $F_j - B_j = 0$, for all j , where $F_j(B_j)$ is the number of forward (backward) events in $|\cos\theta|$ bin j .

^{7b}To be explicit: no χ^2 probability was less than 5%.

^{8a} $R = (F - B)/(F + B)$, where F (B) is the number of events in the forward (backward) hemisphere.

^{8b}If A_G and $A_{\bar{G}}$ are the G -conserving and G -violating amplitudes, respectively, then inspection of the Argand diagram reveals $R \sim 2 A_G A_{\bar{G}} / |A_G|^2$, where R is evaluated for some polar solid-angle element, and where the effect of incoherence and of averaging over

helicities has been ignored.

⁹R. R. Burns, P. E. Condon, H. Kim, M. A. Mandelkern, L. R. Price, and J. Schultz, *Phys. Rev. D* 7, 1310 (1973).

¹⁰R. R. Burns, P. E. Condon, J. Donahue, M. A. Mandelkern, and J. Schultz, *Nucl. Phys.* B27, 109 (1971).

¹¹A. Accensi, V. Alles-Borelli, B. French, A. Frisk, J. M. Howie, W. Krischer, L. Michejda, W. G. Moorhead, B. W. Powell, P. Seyboth, and P. Villemoes, *Phys. Lett.* 20, 557 (1966).